Proceedings of International Conference on Heat Exchanger Fouling and Cleaning - 2015 (Peer-reviewed)
June 07 - 12, 2015, Enfield (Dublin), Ireland
Editors: M.R. Malayeri, H. Müller-Steinhagen and A.P. Watkinson

Published online
www.heatexchanger-fouling.com

# EMBAFFLE® IN REFINERY SERVICE. ON-FIELD STUDY AND DATA VALIDATION THROUGH SMARTPM®

**M. Brignone[1], F. Perrone[1], M. Rottoli[1], S.J. Pugh[2] and E.M. Ishiyama[2]**

[1]EMbaffle B.V., Via Villino 1, 24030 Valbrembo (BG), Italy
[2]IHS Energy, 133 Houndsditch, EC3A 7BX London, United Kingdom
*E-mail: info@embaffle.com

## ABSTRACT

EMbaffle® heat exchangers were introduced to refineries initially by Shell® in 2004 to minimize fouling-related losses in the crude preheating unit. Working in partnership with IHS, operating data have been analyzed to evaluate the effective fouling behaviour of the EMbaffle® technology. This was made possible by the recent implementation of mathematical models of EMbaffle® technology in the IHS heat exchanger network analysis software, SmartPM.

This manuscript is divided into three sections describing, (i), the external flow pattern along an EMbaffle bundle based on a CFD analysis, (ii) analysis of field data and (iii) performance evaluation. In the SmartPM analysis monitoring data collected over ~ 9 months were analysed for a preheat train where a segmental baffle unit was retrofitted to an EMbaffle® unit. Dynamic operating conditions were evaluated to investigate the fouling behaviour. The retrofit bundle equipped with EMbaffle® had a significantly lower fouling rate compared to the segmental baffle unit, even when processing a high fouling blend.

## INTRODUCTION

Heat exchangers are essential components in process industries. When the associated streams are prone to fouling, the thermal-hydraulic performance of exchangers can deteriorate with time. The types of exchangers used depend on the application. In petroleum refineries, conventional segmental baffle exchangers could be used to provide majority of the heat transfer services, but with understanding of flow and fouling behaviour within a unit, advanced designs are identified to be able to better address specific service related issues.

Fouling is a dynamic process and the degree of fouling is strongly influenced through the operating conditions such as the surface temperatures and shear stresses (e.g. for crude oil, Ebert and Panchal, 1997). With increased understanding of dynamic fouling behaviour, better exchanger designs and operating conditions to minimize fouling have attracted considerable attention (e.g. design methods for segmental baffle exchangers, Poddar and Polley, 2000).

The conventional single-segmental baffle design could be further improved through converting the shell-side pressure drop to increase in heat transfer coefficient. For segmental baffle exchangers, part of the shell-side pressure drop is related to the change in direction of stream flow and dead zones due to recirculation of the flow. EMbaffle® is a proprietary technology which eliminates dead zones and the change in shell-side flow when passing through baffles.

### *EMbaffle® Technology in Crude Preheating*

EMbaffle realizes a longitudinal flow configuration (Fig. 1) permitting to sensibly reduce shell-side pressure drop as well as fouling deposition and accumulation. Tubes are supported by special baffles shaped from expanded metal plates, allowing to break the fluid boundary layer with a positive effect on heat transfer.

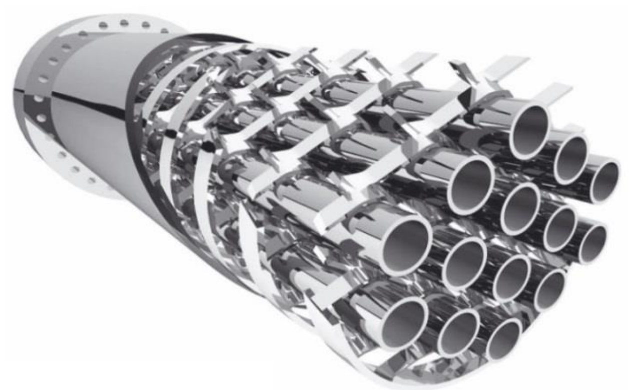

Fig. 1 Schematic representation of a section of EMbaffle heat exchanger. Tube bundle is supported via equally spaced expanded metal baffles.

In the work of van der Zijden *et al*. (2013) a performance comparison between EMbaffle and segmental exchangers operating in parallel trains was presented over a time period of 1.5 years. Analysis of the data showed better performances of EMbaffle in terms of higher overall heat transfer and lower fouling build-up.

Due to its low shell-side pressure drop EMbaffle can be designed in a very effective way, scoring high velocities on the shell-side to achieve a higher external heat transfer coefficient (HTC) than a segmental exchanger under the same available pressure drop. Moreover, due to the elimination of dead zones, uniform flow pattern on the shell-side is achieved resulting in a stable HTC over the longitudinal length.

The manuscript consists of three sections. The first section gives a brief description of a CFD simulation on an EMbaffle geometry, performed to verify the flow pattern on the external tube-bundle. The second section describes data collection of single-segmental baffle unit and EMbaffle unit to evaluate fouling behaviour based on their operating conditions. The third section describes performance comparison of single-segmental baffle and EMbaffle unit in terms of cleaning frequencies and performance deterioration due to fouling on the shell-side.

## CFD SIMULATIONS

### *Governing equations*

The fluid flow in the (three-dimensional) EMbaffle configuration was modelled using CFD Software ANSYS FLUENT. The governing continuity and incompressible, steady state Navier-Stokes equations for a Newtonian liquid are:

$$Continuity: \nabla \cdot v = 0 \tag{1}$$

$$Navier - Stokes: \rho v \cdot \nabla v = -\nabla p + \mu \nabla^2 v + \rho g \tag{2}$$

Here $v$ is the velocity vector, $p$ is the pressure, $\mu$ is the dynamic viscosity, $\rho$ is the density and $g$ is the gravitational acceleration. For simplicity, $g$ was taken as zero.

### *Model setup*

EMBaffle tube-bundle with single flow pass on the shell-side, consisting of a flow distributor and equally spaced EMBaffles was constructed employing a Cartesian coordinate axis highlighted in Fig. 2(a) and (c).

### *Meshing and convergence*

The grids used in the simulation were generated using the internal mesh generator in ANSYS software. The domain was represented using prism and tetrahedral elements.

### *Results from CFD Simulations*

The existence of the annular distributor at the nozzle inlet almost totally eliminates the dead zones typical of the inlet chamber of a segmental baffle unit. Similar considerations apply to the outlet region of the exchanger. Moreover, in the observed flow pattern through the EMbaffle bundle (Fig. 2(b)), the negative velocity profiles are not visible along the longitudinal flow direction. The CFD study was performed to verify that the EMbaffle open structure allows to make a better use of the heat transfer surface area along the running time of the exchanger.

## CASE STUDY ON FIELD DATA COLLECTION

In the case of a bundle replacement for an existing single-segmental baffle exchanger, EMbaffle can be designed as a three-shell-pass, to effectively convert the available pressure drop to enhanced shell-side heat transfer without shell or piping modifications (e.g. Fig. 3).

The case study described hereon refers to the analysis of field data from a crude preheat train in operation in a European refinery. Operational data were monitored continuously and recorded every 8 hour interval. The plant processes a heavy fouling crude blend and the exchanger performances were observed to deteriorate significantly during operation. A single segmental baffle unit was in operation for several years immediately after the pre-flash column was replaced with an EMbaffle three-shell-pass retrofit bundle, allowing almost the same number of tubes as the conventional design. As the number of tube-passes was maintained in the EMbaffle design, tube-side heat transfer coefficient and pressure drop at design conditions did not change to an appreciable extent.

The purpose of the retrofit was to increase the performance of the exchanger (and therefore of the whole section) by enhancing the shell-side heat transfer coefficient (crude-side) and reducing its fouling tendency. Analysis of the data was performed using IHS SmartPM® Software.

## MODEL DESCRIPTION FOR CASE STUDY

### *Data reconciliation*

Data reconciliation fits the monitoring data (temperature and flow measurements) to a physical model (mass and energy balance). Any missing stream flows or temperatures are generated during this process together with the exchanger operational parameters (e.g. film transfer coefficients, Reynolds numbers, film temperatures of cold and hot streams, fouling resistances, etc.). A description of the data reconciliation methodology is detailed elsewhere (Ishiyama et al., 2011, 2013).

### *Heat transfer and pressure drop*

The heat exchanger is situated downstream of the pre-flash column following a booster pump, where the crude stream is maintained at single-phase flow. Assuming fouling is only on the crude-side (shell-side), the overall heat transfer coefficient of a unit, $U$, is given via:

$$\frac{1}{U} = \frac{1}{h_o} + R_{f,o} + \frac{d_o ln\left(\frac{d_o}{d_i}\right)}{2\lambda_w} + \frac{d_o}{d_i}\frac{1}{h_i} \tag{3}$$

Here $h_o$ is the external film transfer coefficient and $h_i$ is the internal film transfer coefficient, $R_{f,o}$ is the external fouling resistance, $\lambda_w$ is the wall thermal conductivity, $d_i$ and $d_o$ are the internal and external tube diameters, respectively. $h_i$ is calculated for laminar, transient and turbulent flow using empirical correlations (ESDU, 1992, 2001). $h_o$ for single segmental baffle exchanger is calculated using a modified stream analysis method based on ESDU (1984). $h_o$ for the 3 shell-side pass EMBaffle is calculated using EMBaffle equations (Reference to EMBaffle internal report).

Shell-side pressure drops for single segmental baffles are calculated using modified stream analysis method based on (ESDU, 1984). Shell-side pressure drop and shear stress for 3 shell-side pass EMBaffle is calculated using EMBaffle equations. The equations are confidential and are not detailed in this manuscript.

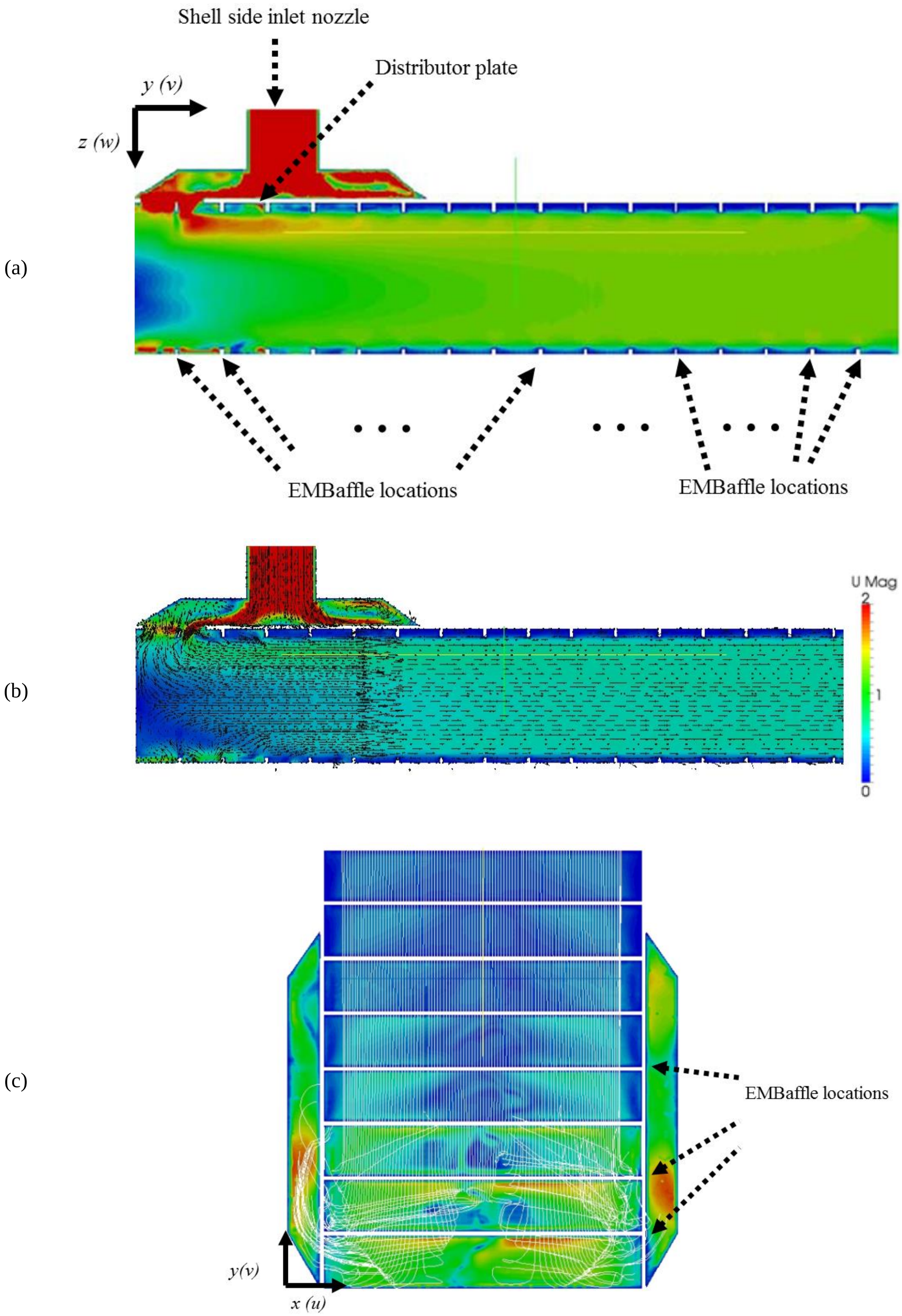


Fig. 2 Velocity field in the tube bundle coloured according to the velocity magnitude. (a) longitudinal cross section of EMBaffle with velocity field, (b) direction of velocity vector, and (c) flow field through cross section of the EMBaffle bundle immediately below the flow distributor.

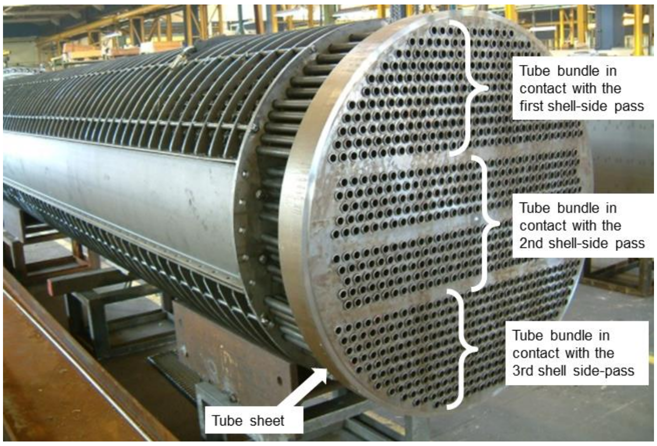

Fig. 3 EMbaffle three-shell-pass bundle.

***Fouling model***
The crude is assumed to undergo chemical reaction fouling. Ebert and Panchal (1997) reported a dynamic fouling model for the crude when the crude is on the tube-side. A generalized form of this model to predict fouling on both the tube- or shell-side fluid is given by (Polley, 2010):

$$\frac{dR_f}{dt} = \frac{a_1}{h} exp\left(-\frac{E}{RT}\right) - a_2\tau \tag{4}$$

Here $a_1$ and $a_2$ are dimensional constants, $h$ is the film transfer coefficient of the fouling stream, $E$ is the activation energy, $R$ is the gas constant, $T$ is the film temperature and $\tau$ is the surface shear stress. The activation energy is assumed as 44.3 kJ mol$^{-1}$ (Wiehe, 2008).

***Scheduling cleaning***
Following the initial work by Epstein (1979) systematic method of identifying optimum cleaning cycles for fouling rate processes are widely discussed in literature. For the case study described in this manuscript the exchanger had to be considered in isolation in the absence of the preheat train information. A heuristic approach is utilized to schedule cleaning where the objective is to maximize the total economic benefit over the operating campaign. The objective function is given *via*:

$$obj = C_E \int_0^{t_F} Q_E \, dt - N_c C_{cl} \tag{5}$$

Here $t_F$ is the operating time span (e.g. interval between shutdowns), $Q_E$ is the exchanger duty, $C_E$ is the cost of energy, $N_c$ is the total number of cleaning actions and $C_{cl}$ is the cost of cleaning.

For illustration, we assume a case where the refinery only performs a clean when the expected net benefit of the cleaning action is a multiple of the cleaning cost (recovered over a specified time period). The criteria can be included in a heuristic algorithm such as those described by Smaïli *et al*. (2001). In this method the operating time span is discretised in to $N_p$ number of periods which is divided into sub-periods of cleaning ($\Delta t_{\text{cleaning}}$) and operational ($\Delta t_{\text{operation}}$) times (Fig. 4).

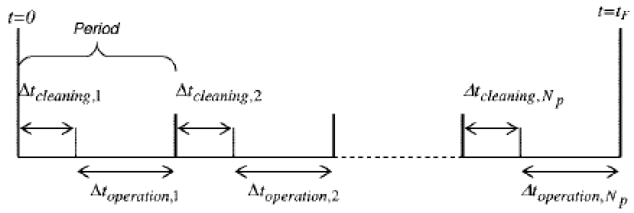


Fig. 4 Time discretisation in formulating the scheduling algorithm.

At the beginning of each period, a simulation is performed to identify the benefit, *B*, of a cleaning action given by:

$$B = C_E \int_t^{t+\Delta tp} \left(Q_{E,with\ clean} - Q_{E,without\ clean}\right) dt - C_{cl} \tag{6}$$

Here subscripts 'with clean' and 'without clean' indicate situations where the exchanger has undergone cleaning and the exchanger not cleaned, respectively. t indicates the beginning of a time period $\Delta t_p$ is the period of expected return of investment.

A cleaning is performed when

$$B > expected\ return \tag{7}$$

The expected return is usually a multiple of the cost of cleaning.

**DATA COLLECTION**
The case study exchanger is located immediately downstream of the pre-flash column. The crude is on the shell-side of the exchanger and is heated via a lower circulating reflux (LCR) stream flowing on the tube-side. The LCR stream has a bypass across the exchanger (Fig. 5). The crude stream inlet and outlet temperatures are measured *via* monitoring tags 'Tc in' and 'Tc out' respectively. The inlet temperature of the LCR stream is measured immediately before the bypass. The temperature of the LCR stream immediately after the exchanger is measured *via* tag 'Th out1'. The mixed LCR stream temperature after the bypass is measured *via* tag 'Th out2'. The crude stream flow across the exchanger is measured *via* tab 'Fc'. The LCR stream flow rate across the exchanger is not measured. The total LCR stream flow before the bypass is measured *via* tag 'Fh'.

Monitoring data for single-segmental baffle unit was collected over a period of 9 months. The unit was then replaced with an equivalent EMBaffle design and the monitoring data were recorded for a period of 8.5 months.

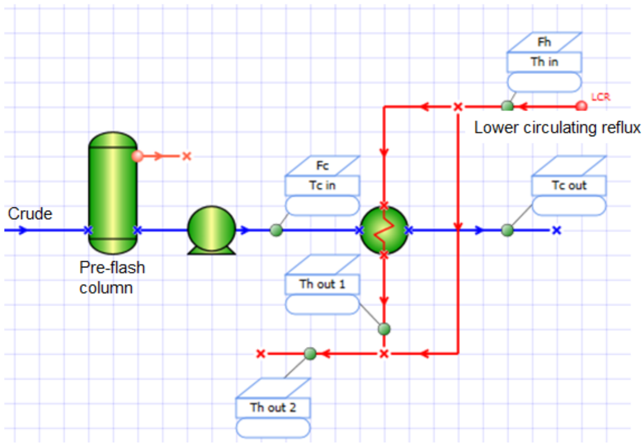


Fig. 5 Illustration of heat exchanger instrumentation. $F_c$ and $F_h$ are cold and hot stream flow measurements, respectively. $T_c$ and $T_h$ are cold and hot stream temperature measurements, respectively. 'in' and 'out' denote inlet and outlet streams.

A straight forward comparison of the single segmental baffle unit and EMBaffle unit was complicated as the inlet conditions for the exchanger were not at controlled conditions. The refinery throughput fluctuated based on the market demand and operational changes elsewhere in the plant. The operating crude and LCR flowrates when data for the single segmental baffle was collected were no longer the same when EMBaffle service was installed. This is reflected in the throughputs and inlet temperature conditions compared in Fig. 6 for single segmental baffle unit and Fig. 7 for EMBaffle unit.

The operating parameters including heat duty, fouling resistance, shell-side equivalent shear stress, external film transfer coefficient and shell-side pressure drops are plotted for single segmental baffle (Fig. 8) and EMBaffle (Fig. 9).

The fouling model described in (4) was fitted to the single segmental exchanger data. The fitted parameters are shown in Table 1. At this stage, the fouling model was only fitted to evaluate the thermal performance. The hydraulic performance would need to be considered in future model developments; particularly when the pressure drop measurements would be available.

Table 1: Fouling model parameters

| Parameter | Value |
|---|---|
| $a_1$ | 550 $h^{-1}$ |
| $a_2$ | $500 \times 10^{-9}$ $m^2K\ J^{-1}\ Pa^{-1}$ |
| $E$ | 44.3 $kJ\ mol^{-1}$ |

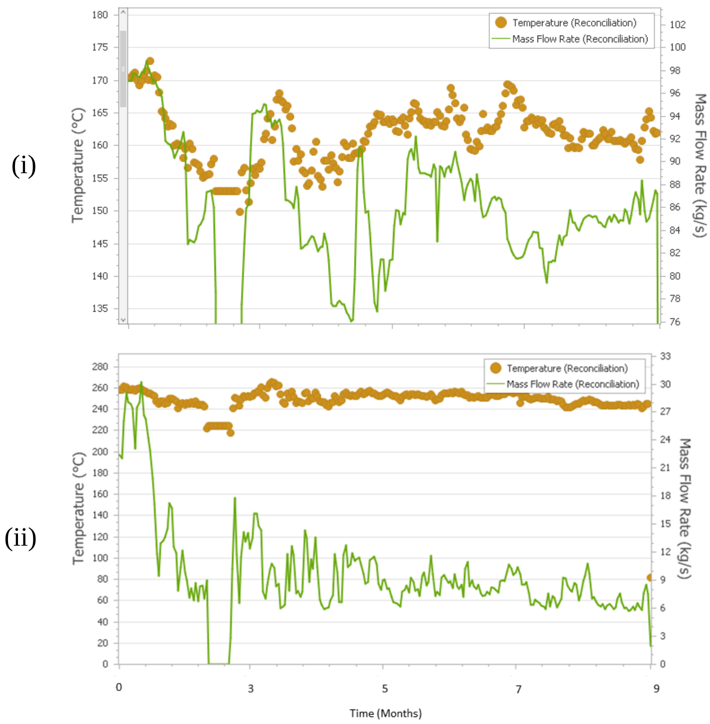


Fig. 6 Reconciled data for segmental baffle exchanger. Inlet temperature and mass flow rate profiles of (i) crude stream and (ii) LCR stream.

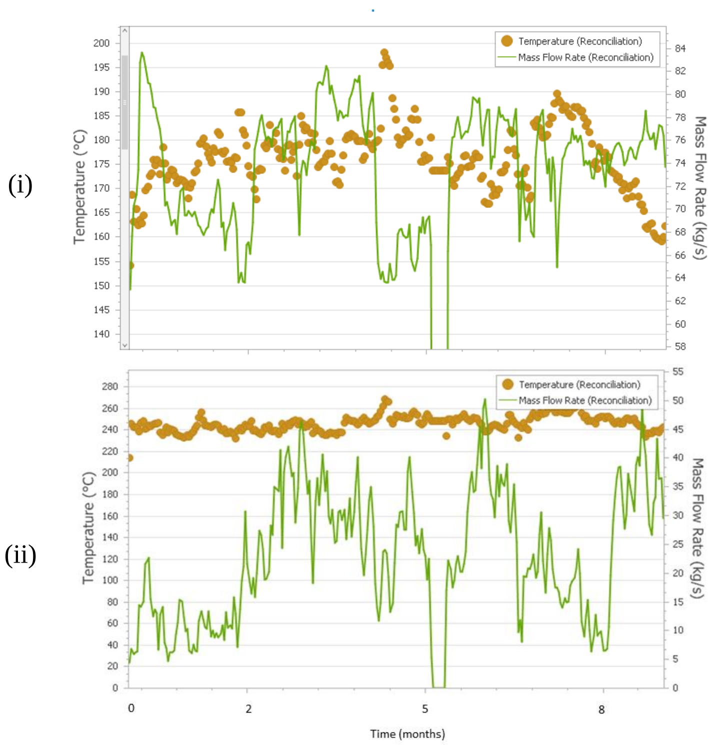


Fig. 7 Reconciled data for EMbaffle exchanger. Inlet temperature and mass flow rate profiles of (i) crude stream and (ii) LCR stream.

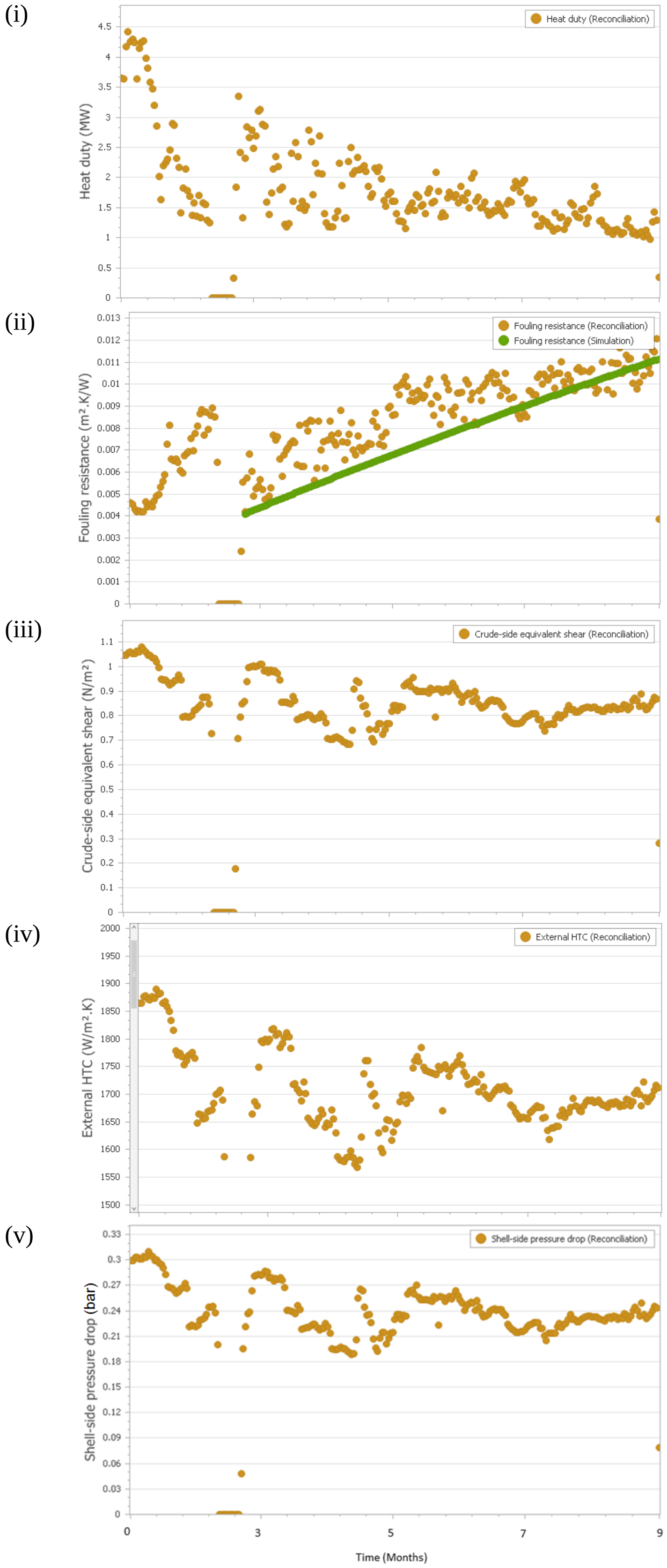


Fig. 8 Operational profiles for single segmental baffle unit: (i) heat duty, (ii) $R_f$, (iii) shear stress, (iv) external transfer coefficient, and (v) shell-side pressure drop.

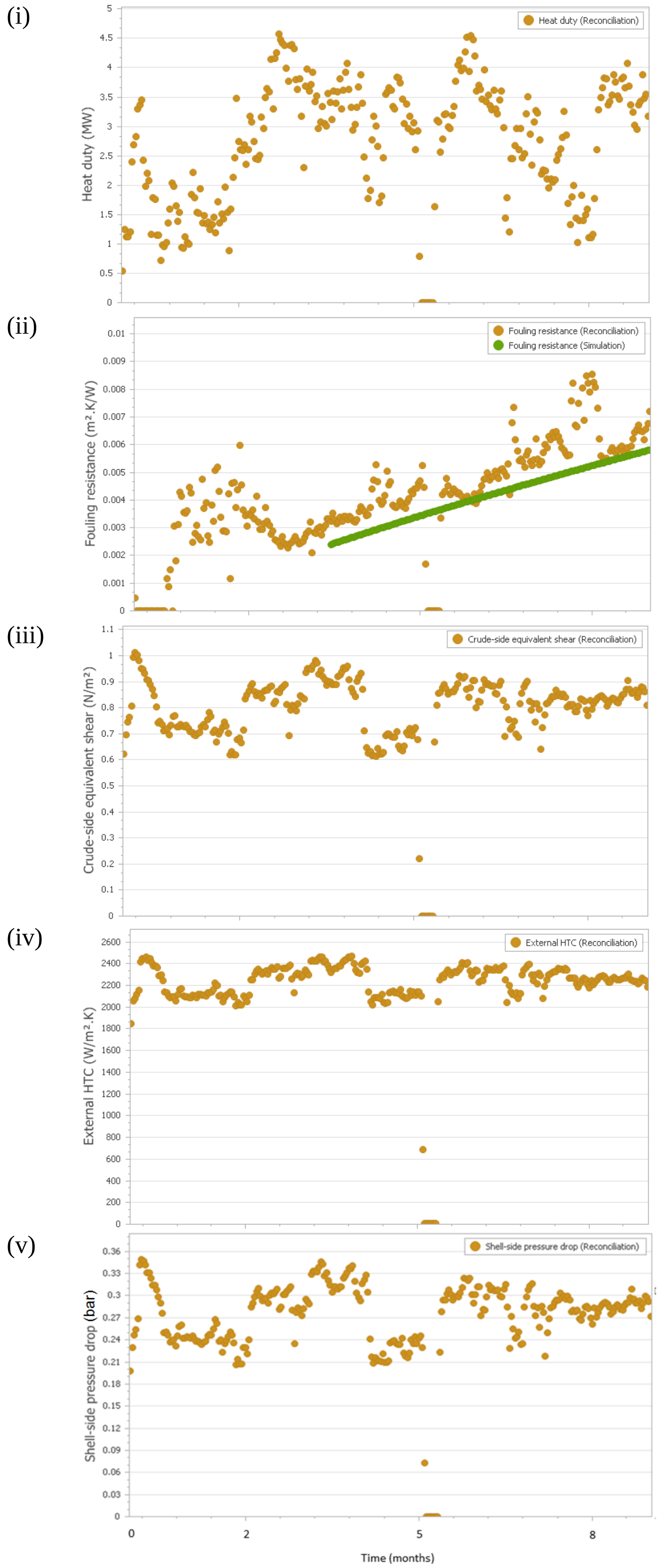


Fig. 9 Operational profiles for EMBaffle unit: (i) heat duty, (ii) $R_f$, (iii) shear stress, (iv) external transfer coefficient, and (v) shell-side pressure drop.

The fit of the fouling model to the plant data is presented by the solid line in the fouling resistance graph, Fig. 8 (ii). Parameters $a_1$ and $a_2$ were then used to fit the EMbaffle data giving the solid line profile in Fig. 9 (ii). This illustrates that the fouling model is fitted for the stream. The rate of fouling is reflected via the operating conditions, i.e. in this example, predominantly by the shell-side film transfer coefficient. The crude-side equivalent shear stress (Fig. 8 (iii) and Fig. 9 (iii)) remains very similar for both the segmental baffle unit and the EMbaffle unit under the operating conditions when the data were collected.

## CLEANING FREQUENCY

For a better comparison of the single-segmental baffle unit and the EMbaffle unit, an optimum cleaning schedule was generated using the algorithm described via equations (5) to (7) using the same inlet conditions described in Table 2.

Table 2*:* Inlet conditions for cleaning scheduling

| | Single segmental baffle | EMbaffle |
|---|---|---|
| LCR flow | 35 kg $s^{-1}$ | |
| Crude flow | 100 kg $s^{-1}$ | |
| LCR inlet temperature | 254.4 °C | |
| Crude inlet temperature | 165 °C | |
| $R_{f,initial}$ ($m^2K\ W^{-1}$) | 0.004 | 0.004 |
| $R_f$ (after cleaning)* ($m^2K\ W^{-1}$) | 0.004 | 0.003 |

*obtained through reconciled data

The degree of cleaning is described via the $R_f$ after cleaning. The value could be extracted from historical $R_f$ profiles. This value is lower for EMbaffles as the EMbaffle geometry enables a much effective cleaning.

The scheduling was performed over a 4 year campaign ($t_F$). The $\Delta t$ and 'expected return' in equations (6) and (7) were taken as 6 months and 100,000 US\$, respectively. The cost of cleaning, Ccl, and the cost of energy $C_E$ were taken as 20,000 US\$ and 6.6 US\$ per MMBtu, respectively. The dynamic fouling model given in (4) with the fouling model parameters obtained in Table 1 were used to simulate the fouling dynamics.

Fig. 10 is a summary of the fouling resistance profile and heat duty for the single segmental baffle unit (denoted in the solid line) and EMbaffle unit denoted in the dashed line. The rate of fouling is notably reduced for the segmental baffle unit. This is reflected via the significantly enhanced external film transfer coefficient and a slightly higher equivalent shear stress under the same operating conditions (Fig. 11(i) and (ii)). The tube-side film transfer coefficient increases slightly with fouling (Fig. 11 (iii)) as the tube-side fluid (LCR stream) becomes hotter reducing its viscosity with fouling on the crude-side.

The net energy recovered (areas of plots in Fig. 10(ii)) is presented in terms of energy economics in Fig. 12. For this case study, the single EMbaffle unit has a total energy benefit of over 600,000 US\$ compared to the single segmental baffle, over the operating campaign with cleaning actions reduced from 3 to 2.

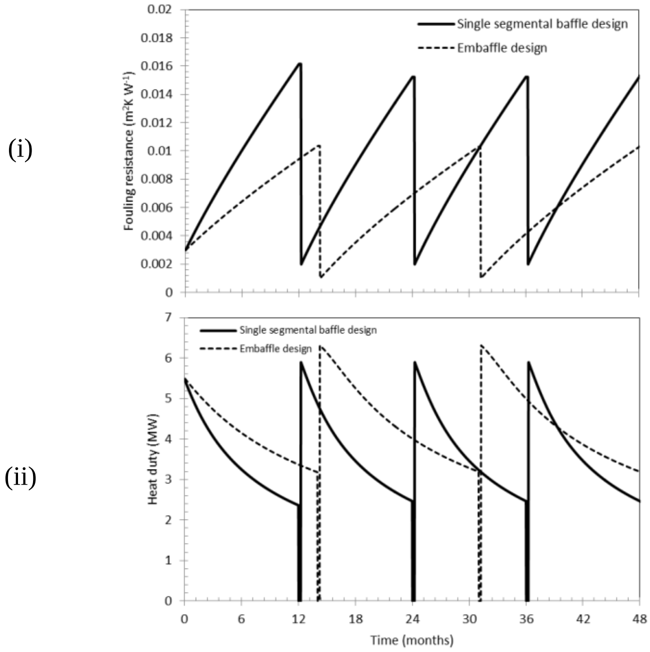


Fig. 10 Comparison of performance for Segmental baffle and EMbaffle units: (i) $R_f$ and (ii) heat duty.

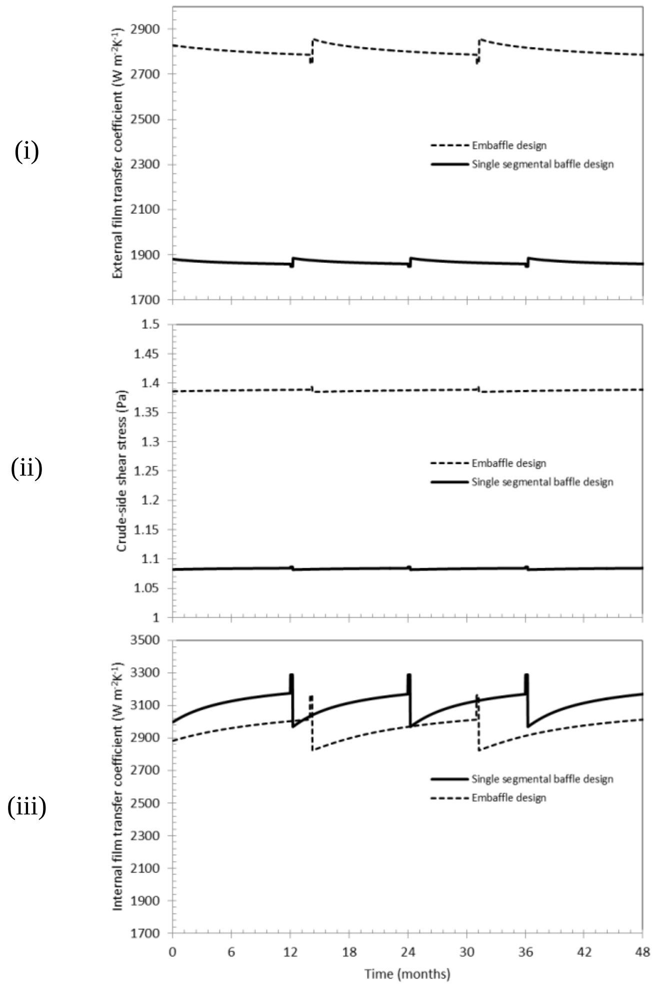


Fig. 11 Profiles of (i) external transfer coefficient, (ii) equivalent crude-side shear and (iii) internal transfer coefficient. Solid and dashed lines represent segmental baffle and EMbaffle heat exchangers, respectively

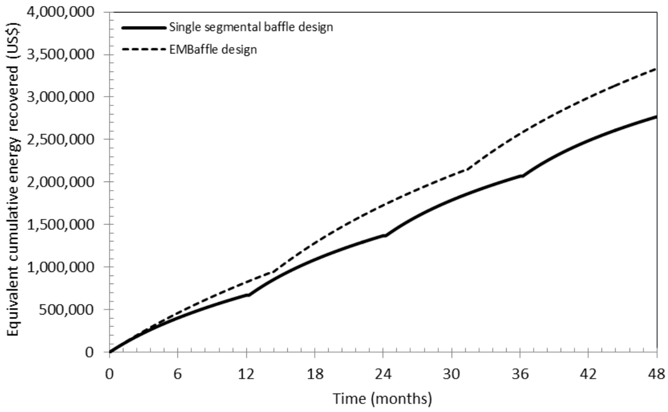


Fig. 12 Profiles of (i) Fouling resistances and (ii) Heat duties. Solid and dashed lines represent single segmental baffle and EMbaffle heat exchangers, respectively.

## CONCLUSIONS

1. Field fouling data for single segmental baffle and EMbaffle designs were collected.
2. A dynamic fouling model to evaluate the thermal fouling behaviour was fitted to the fouling profile obtained from single segmental baffle unit. The same model was able to predict the thermal fouling on the EMbaffle unit. However, the model is open to improvement with the availability of further plant monitoring data including pressure drop measurements (which was not available at this stage).
3. A performance comparison showed reduction in fouling in EMbaffle units due to enhancement of the external film transfer coefficient when the heat transfer is shell-side limited.

## NOMENCLATURE

$a_1$ deposition constant, $h^{-1}$
$a_2$ suppression constant, $m^2K\ J^{-1}\ Pa^{-1}$
$B$ benefit, US$
$C_E$ cost of energy, US$ $J^{-1}$
$C_{cl}$ cost of cleaning, US$ $unit^{-1}$
$d$ tube diameter, m
$E$ activation energy, J $mol^{-1}$
$g$ gravitational acceleration, m $s^{-2}$
$h$ film transfer coefficient, W $m^{-2}K^{-1}$
$N_c$ number of cleaning events, -
$N_p$ number of descritized time periods, -
*obj* objective function value, US$
$p$ pressure, kPa
$Q_E$ energy cost, MW
$R$ gas constant, J $mol^{-1}$ $K^{-1}$
$R_f$ fouling resistance, $m^2$ K $W^{-1}$
$t_F$ operating campaign, s
$\Delta t_{cleaning}$ period when the exchanger is offline, s
$\Delta t_{operation}$ period when the exchanger is in operation, s
$\Delta t_p$ period for expected return, s
$T$ film temperature, K
$U$ heat transfer coefficient, W $m^{-2}$ $K^{-1}$
$u, v, w$ velocity, m $s^{-1}$
$x, y, z$ Cartesian coordinate system

Subscripts
$c$ cold
$h$ hot
$i$ internal
$o$ external
with cleaning with cleaning action
without cleaning without cleaning action

Symbols
$\lambda_w$ thermal conductivity of tube, W $m^{-1}$ $K^{-1}$
$\mu$ dynamic viscosity, Pa s
$\rho$ density, kg $m^{-3}$
$\tau$ shear stress, Pa

## REFERENCES


Ebert, W.A., and Panchal, C.B. (1997). Analysis of Exxon crude-oil slip stream coking data. In Fouling Mitigation of Industrial Heat Exchange Equipment, (New York: Begell House), pp. 451–460.

Epstein, N. (1979). Optimum evaporator cycles with scale formation. Can. J. Chem. Eng. 57, 659–661.

ESDU (1984). Baffled shell-and-tube heat exchangers: flow distribution, pressure drop and heat transfer coefficient on the shellside (London, UK: IHS).

ESDU (1992). Forced convection heat transfer in straight tubes. Part 1: turbulent flow (London, UK: IHS).

ESDU (2001). Forced convection heat transfer in straight tubes Part 2. laminar and transitional flow (London, UK: IHS).

Ishiyama, E.M., Pugh, S.J., Wilson, D.I., Paterson, W.R., and Polley, G.T. (2011). Importance of data reconciliation on improving performances of crude refinery preheat trains. In AIChE Annual Meeting, Conference Proceedings,.

Ishiyama, E.M., Pugh, S.J., Paterson, W.R., Polley, G.T., Kennedy, J., and Wilson, D.I. (2013). Management of crude preheat trains subject to fouling. Heat Transf. Eng. 34, 692–701.

Poddar, T.K., and Polley, G.T. (2000). Optimize shell-and-tube heat exchanger design. Chem. Eng. Prog. 96, 41–46.

Polley, G.T. (2010). Review of the development of models for the prediction of fouling rates in exchangers heating crude oil. (Jersey City, NJ, USA), pp. 13–17.

Smaïli, F., Vassiliadis, V.S., and Wilson, D.I. (2001). Mitigation of fouling in refinery heat exchanger networks by optimal management of cleaning. Energy Fuels 15, 1038–1056.

Wiehe, I.A. (2008). Process chemistry of petroleum macromolecules (US: CRC Press).

Van der Zijden, E.J.J., Brignone, V.M., Rottoli, M., and van Lint, C.F.J.M. (2013). EMbaffle heat exchanger in fouling operation. In Heat Exchanger Fouling and Cleaning, Budapest, Hungary.